Journal of the Korean Nuclear Society
Volume 33, Number 4, pp.397~408, August, 2001

Numerical Study on the Natural Circulation Characteristics in an Integral Type Marine Reactor for Inclined Conditions

Tae-Wan Kim and Goon-Cherl Park
Seoul National University
San 56-1, Shinlim-dong, Kwanak-gu, Seoul 151-742, Korea
Jae-Hak Kim
Future and Challenge Co., LTD.
130-202, San 56-1, Shinlim-dong, Kwanak-gu, Seoul 151-742, Korea
taewan1@snu.ac.kr

(Received February 22, 2001)

Abstract

A marine reactor shows very different thermal-hydraulic characteristics compared to a land-based reactor. Especially, study on the variation of flow field due to ship motions such as inclination, heaving and rolling is essential since the flow variation has great influence on the reactor cooling capability. In this study, the natural circulation characteristics of integral type marine reactor with modular steam generators were analyzed using computational fluid dynamics code, CFX-4, for inclined conditions. The numerical analyses are performed using the results of natural circulation experiments for integral reactor which are already conducted at Seoul National University. From the results, it was found that the flow rate in the ascending steam generator cassettes increases due to buoyancy effect. Due to this flow variation, temperature difference occurs at the outlets of the each steam generator cassettes, which is mitigated through downcomer by thermal mixing. Also, around the upper pressure header, the flow from descending hot leg goes up to the ascending steam generator cassettes due to large natural circulation driving force in ascending steam generator cassettes. From this result, the increase of flow rate in the ascending steam generator cassettes could be understood qualitatively.

Key Words : marine reactor, integral reactor, natural circulation, inclined condition, CFX-4 modular steam generator.

1. Introduction

Small and medium integral reactors are expected to be widely used in the various fields such as seawater desalination, district heating and ship propulsion. Keeping in step with this expectation, integral reactors have been developed in many countries[1-2]. In England, the conceptual design of SIR(Safe Integral Reactor) is already completed. In Japan, SPWR(System-integrated

Pressurized Water Reactor) has been developed by JAERI(Japan Atomic Energy Research Institute) since 1983. In Russia, OKBM(Research and Design Bureau of Machine Building) takes a lead in the development of VPBER-600. The conceptual design for nuclear system, turbine and automatic process control system for VPBER-600 has been completed and the real design is in progress. Also, KAERI(Korea Atomic Energy Research Institute) has developed a small and medium scale integral reactor, SMART(System-integrated Modular Advanced ReacTor)[3].

There have been many efforts to use nuclear power as a power source for ship. In Japan, the first Japanese nuclear ship, Mutsu, was constructed in 1969[4]. Also, JAERI has developed MRX(Marine Reactor X) and DRX(Deep-sea Reactor X) as a power source of an icebreaker and a bathyscaphe, respectively. Studies on the safety of nuclear ship Savannah[5], Otto-hahn[6] and Lenin have been performed by the USA, Germany and Russia, respectively.

The marine reactor always experiences ship motions due to sea condition. Therefore, in designing a marine reactor, it is very important to evaluate the effects of ship motion on the thermal-hydraulics of the reactor coolant system. Especially, it is important to evaluate such effects for natural circulation condition because natural circulation is the only way to remove the residual heat after accidents. During the natural circulation operation for residual heat removal after accidents, the primary coolant distribution can be seriously influenced by ship motions. In Japan, studies on the effects of heaving[7-9], inclination[10-11], and rolling[12] have been performed. However, the inclination test facility of JAPAN has a simple SG(Steam Generator) which has an annular flow area and is located around the core. And, no previous research has been done on the natural circulation characteristics of the integral type marine reactor with modular SG cassettes, which is the design feature of SMART.

Table 1. Initial Conditions of Experiment

Initial Condition	30°	45°
Pressure (MPa)	0.1	0.1
Core Power (kW)	72	72
Primary Temperature (℃)	9.8	9.8
Secondary Temperature (℃)	9.8	9.8
Secondary Flow Rate per each SG cassette (m^3/sec)	1.0×10^{-4}	1.0×10^{-4}

This study focuses on the investigation of the natural circulation characteristics in integral-type marine reactor for inclined conditions. Steady state natural circulation test had been performed using an experimental facility. And the three dimensional flow field was analyzed using the computational fluid dynamics code, CFX- 4[13] to evaluate the asymmetric flow patterns and thermal mixing phenomena in the UPH(Upper Pressure Header) and downcomer.

2. Experiment

2.1. Experimental Facility

To investigate the thermal-hydraulic characteristics in integral type marine reactor during natural circulation operation, the single-phase natural circulation tests for inclined conditions were performed using experimental facility of SMART, SEA (SMART Experimental Apparatus)[14]. SEA is a scaled model of integral reactor SMART. The scaling methods suggested by Ishii[15] and Kocamustafaogullari[16] were used. However, exact scaling is not important in this experiment because the objective of this experiment is to investigate the fundamental characteristics of general marine reactor having modular SG cassettes. The length and the flow

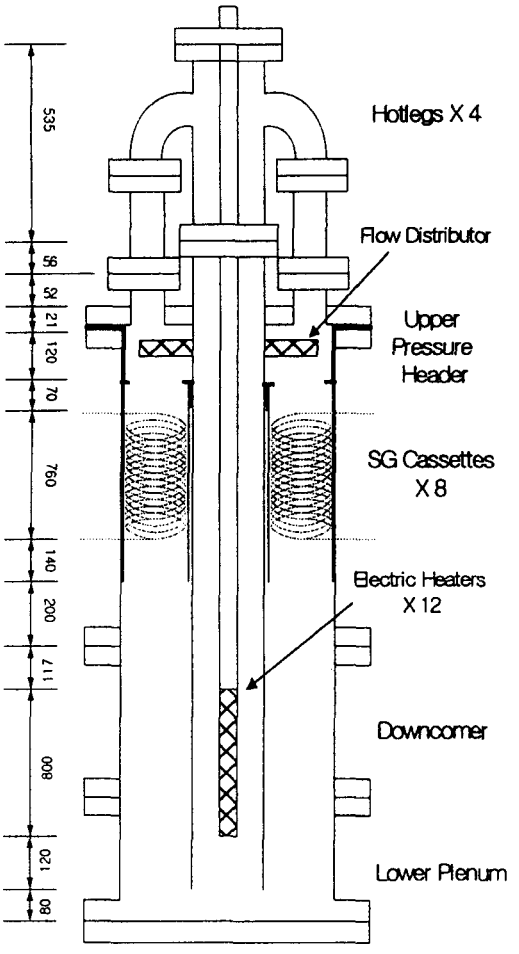

Fig. 1. Schematic Diagram of SEA

area are scaled down to 1/2.5 and 1/80, respectively. Maximum core power is set as 72 kW to consider the decay heat and the volume ratio between the prototype and model. The initial conditions for 30° and 45° inclination are summarized in Table 1.

SEA consists of twelve electric heaters, four hot legs, UPH, eight once-through type SG cassettes and downcomer as shown in Fig. 1. Also, there is a secondary coolant system which supplies a constant secondary feedwater flow. The primary coolant passes through the core, four hot legs, the UPH, which is designed to make uniform flow into the SG cassettes, eight SG cassettes and the downcomer, in sequence. Also, SEA is mounted on the leaning equipment for inclination as shown in Fig. 2. With a 15° increment, the inclination angle can be changed from 0° to 75°. The left bottom of Fig. 2 is the top view of SEA showing the location of the hot legs and SG cassettes. Hot leg 1, SG 1 and SG 8 are located at the left and go downward during inclination. The natural circulation tests were performed for 0°, 15°, 30° and 45° inclinations.

Fig. 2 also shows the measuring instruments and their positions. During the test, flow rate, temperature and pressure difference are measured and the measured data are processed by data acquisition system, HP3852. For measuring the total natural circulation flow rate in each hot leg the paddle-type magnetic flow meter that has ±1% full-scale error is used. To investigate the primary coolant cooling and thermal mixing phenomena, temperatures are measured with T-type thermocouple at the inlet and outlet of each SG cassette, 150 mm below of each SG outlet and bottom of downcomer. Since the measurement of the core temperature is difficult and there is no heat sink in the region from core to hot leg, the hot leg temperature can represent the core temperature. To measure the heat removal rate of each SG cassette, the temperatures at the inlet and outlet of secondary side are measured. Also, the natural circulation flow rate of each SG cassette can be calculated from heat balance between primary and secondary sides. Pressure differences between the inlet and outlet of each SG cassette are measured with wet-wet differential pressure transducer, DP103, to provide input data for CFX-4 calculation.

2.2. Summary of Test Results

As the inclination angle increases, the total

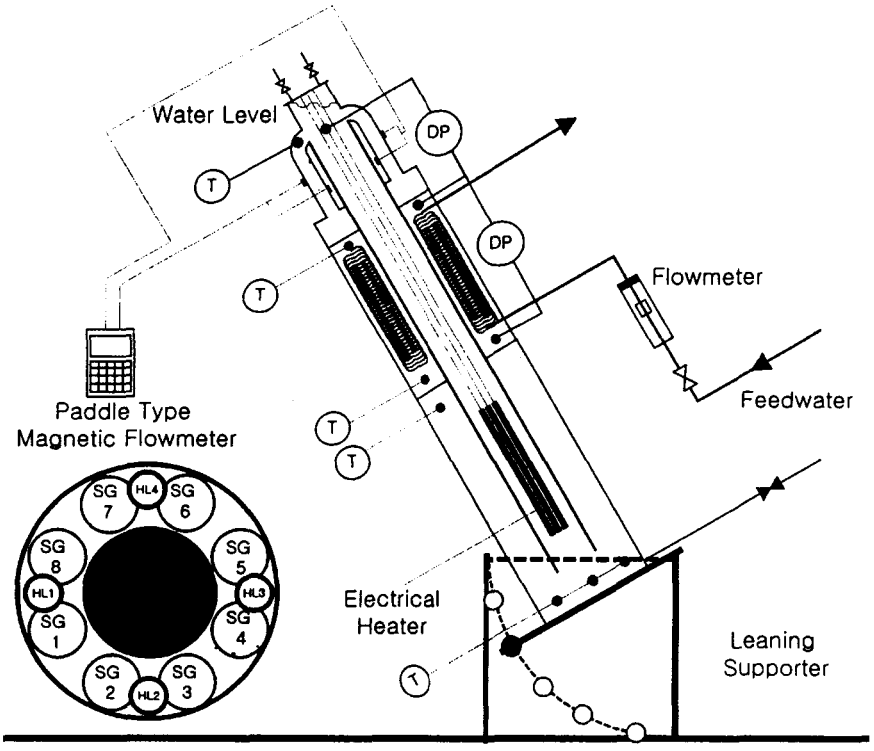

Fig. 2. Configuration and Instrumentation of SEA

natural circulation flow rate is decreased by the decrease of elevation difference between core and SG cassettes. Also, it is found that the difference of flow rate in each hot leg is almost negligible and has nothing to do with inclination. However, the flow rate in ascending SG cassette is increased. The flow rate in each SG cassette can be calculated from the heat balance between the primary and secondary sides of SG cassette.

The core temperature is increased by the decrease of total flow rate. Since the flow rate in ascending SG cassette is increased, the heat removal rate is also increased in ascending SG cassette. However, since the secondary feedwater flow rates are equal for all SG cassettes, the heat removal rate in ascending SG cassette cannot be increased as much as the flow rates of the primary coolant. Therefore, the temperature at the ascending SG cassette outlet is much higher than that of descending SG cassette. But such temperature difference can be mitigated by the thermal mixing in the downcomer.

Pressure drop in the SG cassette consists of pressure drops due to buoyancy and friction[17]. From the result of the experiment, it can be deduced that the pressure drop due to buoyancy is dominant in the SG cassette and that due to friction is negligibly small.

The details of experiments can be found in reference[14].

3. Numerical Analysis Using CFX-4

3.1. Modeling

The three-dimensional effect due to inclination

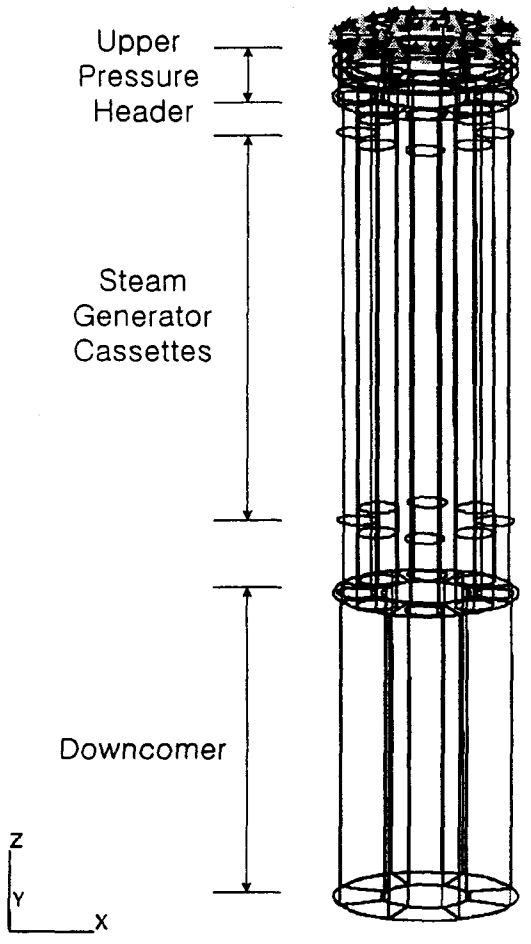

Fig. 3. Front View of the Geometry

plays an important role in the distribution of the primary coolant in the region from the UPH to the downcomer. Therefore, in this study, the region from the UPH to the downcomer is determined as the calculation domain. For this, the geometry with multi-block structure is created with CFX-Build[18] which is the pre-processor of CFX-4 code as shown in Figs. 3 and 4. The geometry consists of three parts which are the UPH, SG part and downcomer. The SG part is treated with porous media because it is very difficult to model the helical coil in each SG cassette exactly, and also the secondary side is excluded from this geometry. The geometry has four inlets which represent the outlet of each hot leg and single outlet that stands for the bottom of downcomer and consists of total 11,176 cells.

3.2. Governing Equations and Numerical Scheme

CFX-4 uses body-fitted grid, non-staggered grid with Rhie-Chow momentum interpolation, finite volume method and SIMPLE(Semi-Implicit Method for Pressure Linked Equation) algorithm for calculating the governing equations. For the analysis, continuity equation, incompressible three-dimensional Navier-Stokes equation and energy equation are used. Also, standard k- ϵ model is used for turbulent flow analysis. The detailed governing equations with coordinates-free tensor notation are as follows;

Continuity Equation :

$$\frac{\partial(\rho U)}{\partial t} + \nabla \cdot (\rho U) = 0 \tag{1}$$

Momentum Equation :

$$\frac{\partial(\rho U)}{\partial t} + \nabla \cdot (\rho U \otimes U) - \nabla \cdot (\mu_{eff} \nabla U) = -\nabla P' + \nabla \cdot (\mu_{eff} (\nabla U)^T) + B \tag{2}$$

Modified Pressure :

$$P' = P + \frac{2}{3}\rho k + (\frac{2}{3}\mu_{eff} - \zeta)\nabla \cdot U - \rho_0 g \, x \tag{3}$$

Viscosity

$$\mu_{eff} = \mu + \mu_T$$
$$\mu_T = C_\mu \rho \frac{k^2}{\varepsilon} \tag{4}$$

Transport Equation for Turbulence Kinetic Energy :

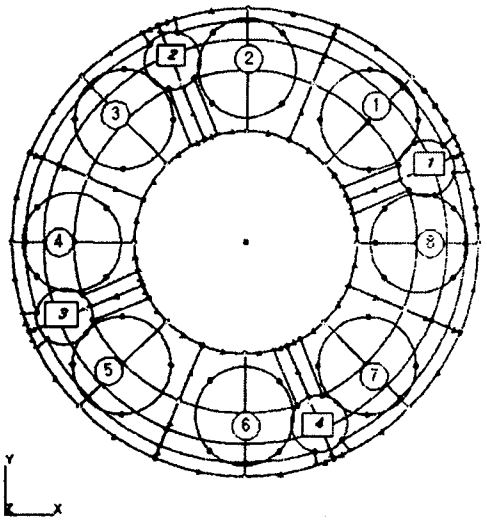

Fig. 4. Top View of the Geometry

$$\frac{\partial(\rho k)}{\partial t}+\nabla\cdot(\rho U k) - \nabla\cdot\left[(\mu+\frac{\mu_T}{\sigma_k})\nabla k\right]=P_s+G-\rho\varepsilon \tag{5}$$

Transport Equation for Turbulence Dissipation Rate :

$$\frac{\partial(\rho\varepsilon)}{\partial t}+\nabla\cdot(\rho U\varepsilon)-\nabla\cdot\left[(\mu+\frac{\mu_T}{\sigma_\varepsilon})\nabla\varepsilon\right] = C_1\frac{k}{\varepsilon}[P_s+C_3\max(G,0)]-C_2\rho\frac{\varepsilon^2}{k} \tag{6}$$

Shear Production :

$$P_s=\mu_{eff}\nabla U\cdot\left[\nabla U+(\nabla U)^T\right] -\frac{2}{3}\nabla\cdot U\left(\mu_{eff}\nabla\cdot U+\rho k\right) \tag{7}$$

Production due to the Body Force :

$$G=-\frac{\mu_{eff}}{\rho\sigma_\rho}g\cdot\nabla\rho \tag{8}$$

Energy Equation :

$$\frac{\partial(\rho H)}{\partial t}+\nabla\cdot(\rho U H)-\nabla\cdot(\lambda\nabla T)=0. \tag{9}$$

For porous media assumption for SG parts, the modified continuity, Navier-Stokes and energy equations are used.

Continuity Equation for Porous Media :

$$\frac{\partial(\gamma\rho)}{\partial t}+\nabla\cdot(\rho K\cdot U)=0 \tag{10}$$

Momentum Equation for Porous Media :

$$\frac{\partial(\gamma\rho U)}{\partial t}+\nabla\cdot(\rho(K\cdot U)\otimes U) -\nabla\cdot(\mu_{eff}K\cdot(\nabla U+(\nabla U)^T) =-\gamma R\cdot U-\gamma\nabla p \tag{11}$$

Energy Equation for Porous Media :

$$\frac{\partial(\gamma\rho H)}{\partial t}+\nabla\cdot(\rho K\cdot UH) -\nabla\cdot(\Gamma_e K\cdot\nabla H)=\gamma(K\cdot U) \tag{12}$$

To improve the convergence in the complex geometry, AMG(Algebraic Multi-Grid) solver is used in the pressure calculation. Also, the upwind scheme[19] is used in the calculations of the k and ε equations to guarantee the positive value of k and ε. For better convergence, the under relaxation factors are used to velocity components, k, ε and enthalpy. The applied under relaxation factor for each variable except enthalpy is 0.3. The applied under relaxation factor for enthalpy is 0.95 which is lager value than those of other terms because the large under relaxation factor leads the solution with the better convergence in the buoyancy-driven flow problem.

3.3. Boundary Conditions

The boundary conditions consist of five parts which are inlet condition, outlet condition, porous media condition for SG parts, heat removal condition in each SG cassette and inclination condition.

For inlet condition, in this study, the velocity calculated from flow rate and the temperature measured in experiment are used. For velocity, it is assumed that velocity has axial component only since axial component is dominant due to narrow flow path. Although temperature is measured at the top of each hot leg, the measured temperature is used for inlet condition because there is no heat sink in the region from the inlet to outlet of hot leg.

At the outlet, flow rate is assumed to be equal to the total flow rate at four inlets. The extrapolated pressure from upstream is used as the outlet pressure.

Since the detailed description for helical coil in each SG cassette is difficult and the secondary side is not modeled, the SG parts are treated as porous media. Due to the porous treatment of SG cassettes, two additional boundary conditions are required, which are the volume porosity and the resistance coefficient. The volume porosity represents the proportion of available flow volume to the total volume. The calculated volume porosity from design document is 0.8197. The resistance coefficient is an input to calculate the frictional pressure drop through porous media. However, it is found from the experimental results that there is too small frictional pressure drop and it can be neglected. Therefore, in this calculation, the resistance coefficient is set as zero.

Because the secondary side modeling is excluded from this analysis, an additional boundary condition is required for the modeling of heat removal in SG cassette. For modeling of heat removal phenomena, it is assumed that the heat is removed uniformly in SG cassette. Actually, since the SG cassette of SEA is a once-through type and the primary and secondary coolant flows as a counter-current, the heat is removed uniformly in SG cassette of SEA. Based on uniform heat removal in SG cassette, the total heat removal rate in each SG cassette is considered as the source term in energy equation which is a negative value. Also, the heat removal rate in each SG cassette is calculated from the secondary flow rate and the temperature difference between inlet and outlet of secondary side.

The components of gravity vector are varied with the inclination angle. Since hot leg 1, SG 1 and SG 8 go downward by inclination and hot leg 1 is located at the position of $+22.5^\circ$ from x-axis in Fig. 4, the gravity vector at the inclination angle, θ, can be calculated as

$$\vec{g} = (9.8\cos 22.5^\circ \sin\theta,\ 9.8\sin 22.5^\circ \sin\theta,\ -9.8\cos\theta) \quad (13)$$

The detailed boundary conditions are listed in Table 2.

4. Results

4.1. Flow Rates

In the experiments, the flow rates in the ascending SG cassettes 4 and 5 are larger than those in the descending SG cassettes 1 and 8. This is due to the larger natural circulation driving forces in the ascending SG cassettes than those in the descending SG cassettes since they are induced by the elevation difference between the core and the SG cassettes. In SEA, the elevation differences between the ascending and descending SG cassettes are 3.5 cm and 8.5 cm for 30° and 45° inclinations, respectively.

From the analysis result, it is found that the flow rates in the ascending SG cassettes are increased with augmentation of inclination angle as shown in Fig. 5. Fig. 6 represents the velocity field in the UPH for 45° inclination. In this figure, it can be found that not all of the primary coolant from the descending hot leg 1 passes through the

Table 1. Detailed Boundary Conditions

Condition		30°	45°
Heat Removal Condition in Steam Generator Cassette	Heat removal rate for SG 1(kW)	6.3398	5.2114
	Heat removal rate for SG 2(kW)	7.3667	6.7078
	Heat removal rate for SG 3(kW)	7.0314	6.8713
	Heat removal rate for SG 4(kW)	7.2284	7.7054
	Heat removal rate for SG 5(kW)	7.8865	8.2671
	Heat removal rate for SG 6(kW)	6.8428	6.9845
	Heat removal rate for SG 7(kW)	6.9057	6.3809
	Heat removal rate for SG 8(kW)	6.8512	5.9282
Inclination Condition	Gravity Vector (m/sec^2)	(4.527, 1.875, -8.487)	(6.402, 2.652, -6.930)
Inlet Condition	Velocity (m/s)	9.4392×10^{-2}	7.8145×10^{-2}
	Temperature (℃)	58.16	63.95

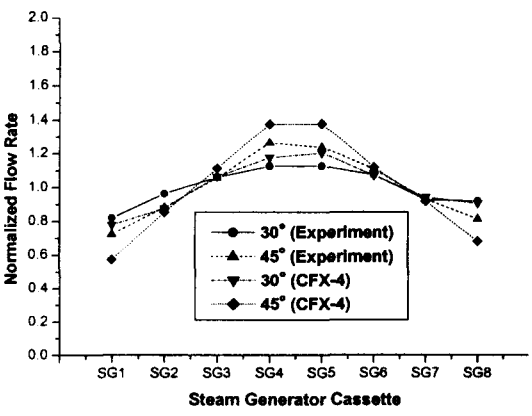

Fig. 5. Normalized Flow Rates in SG Cassettes

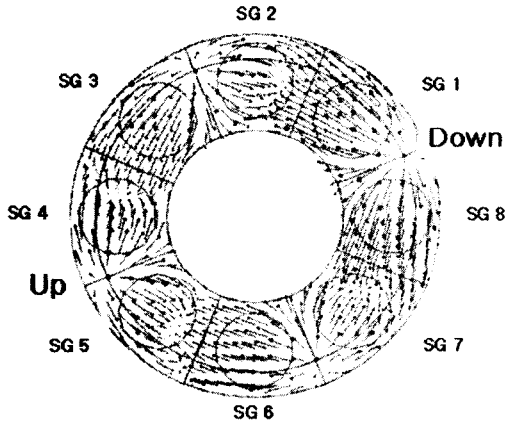

Fig. 6. Velocity Vectors in the UPH

descending SG cassettes located below, but a large amount of the primary coolant goes up to the upper part of the UPH and more coolant goes down into the ascending SG cassettes. This is due to the low frictional pressure drop in each SG cassette. In the analysis, since the frictional pressure drop in the SG cassette is neglected, the flow distribution into the SG cassettes is affected by the buoyancy only. Because the ascending SG cassettes have a larger buoyancy forces, the flow rates in the ascending SG cassettes are increased. As a result of this phenomenon, the primary coolant in the UPH spreads out to the ascending SG cassettes. It can be said that this is a typical natural circulation flow characteristic of an integral type marine reactor with modular SG

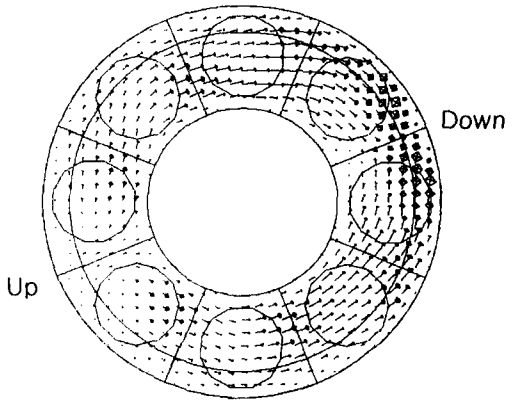

Fig. 7. Velocity Vectors in the Upper Region of the Downcomer

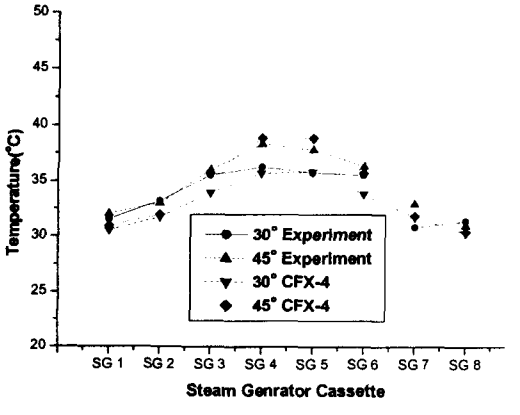

Fig. 8. Temperature in Each SG Cassette Outlets

cassettes.

The velocity field in the upper region of the downcomer is shown in Fig. 7. The primary coolant from the each SG cassette is merged in the downcomer. Due to the inclination, the primary coolant from the ascending SG cassettes is spread to the lower region of the downcomer and mixed with that from the descending SG cassettes as shown in Fig. 7. Since the mixing phenomena continuously occur through the downcomer region, there is uniform flow distribution at the end of the analysis domain.

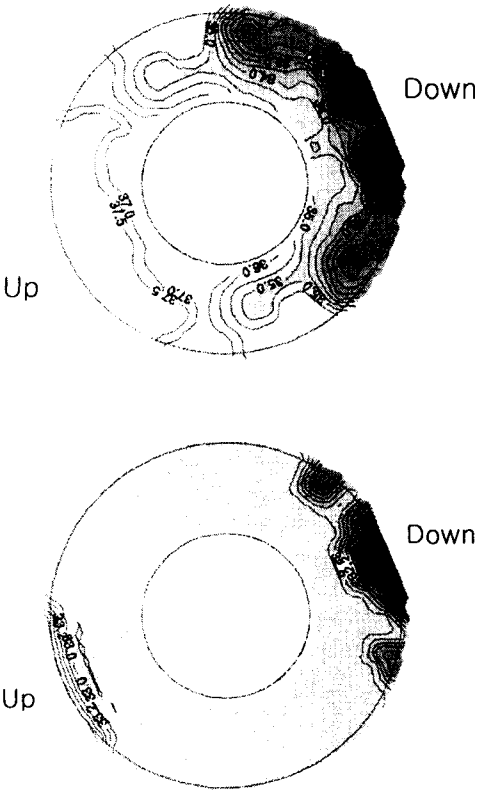

Fig. 9. Downcomer Temperature Distribution for 45° Inclination

Also, the flow mixing in the downcomer plays an important role in mitigating the temperature difference, which will be discussed in the next section.

4.2. Temperature

With the increase of the inclination angle, the temperature difference between ascending and descending SG cassettes is increased as shown in Fig. 8. This result, which coincides with the experimental result, can be explained as follows. In the experiment, since a large amount of the primary coolant is entered to the ascending SG cassettes, the heat removal rates in the ascending

SG cassettes are increased. However, the outlet temperatures of the ascending SG cassettes are higher than those of the descending SG cassettes because of the constant feedwater flow in all SG cassettes. This can be adapted to the numerical analysis. In the analysis, the heat in the ascending SG cassettes cannot be sufficiently removed because the heat removal rate obtained from the experiment is applied as a boundary condition and the flow rate into the ascending SG cassettes is increased as much as that of the experiment. The temperature differences between the ascending and descending SG cassette are 5.6℃ and 8.4℃ for 30° and 45° inclinations, respectively.

As explained in Section 4.1, the primary coolant from each SG cassettes is mixed with each other passing through the downcomer region. From the thermal mixing, the temperature difference between each SG cassette outlets is mitigated by less than 1℃ through the downcomer region and the uniform temperature distribution can be obtained at the end of the analysis domain. The downcomer temperature distribution for 45° inclination in Fig. 9 shows good thermal mixing during inclination.

However, there is a little difference between CFX-4 calculation and experiment. This is due to the SG cassette modeling. As explained in section 3.3, the SG cassette is assumed to porous medium and the heat transfer phenomena between primary and secondary side are given as boundary conditions. Because of this assumption, the flow field in each SG cassette is distorted in CFX-4 calculation and the heat transfer phenomena are rather different from those in experiment. But the result of CFX-4 calculation is very useful to analyze the experimental result because the calculation result has a same trend compared to experimental result and can show the three-dimensional flow field which cannot be found in experimental result.

5. Conclusions

To investigate the three-dimensional natural circulation characteristics in an integral type marine reactor for inclined condition, the numerical analysis based on the single-phase natural circulation test is performed using the computational fluid dynamics code, CFX-4. From the analysis results, the flow rates in the ascending SG cassettes are increased by inclination due to the buoyancy and negligibly low frictional pressure drop. Also, the increase of flow rates in the ascending SG cassettes can be understood qualitatively. From the flow field analysis, the flow mixing phenomena in the downcomer can be understood more accurately. It is also found that the temperature distribution is almost mitigated by the thermal mixing through the downcomer and the temperature at the inlet of the core will be identical even though the temperatures at the outlet of the ascending SG cassettes are higher than those of the descending SG cassettes.

Nomenclature

English

B : Body Force

$C\mu$: Constant in Eddy Viscosity Formula [Default value in standard k-ε model = 0.09]

C_1 : Constant in ε Equation [Default value in standard k-ε model = 1.44]

C_2 : Constant in ε Equation [Default value in standard k-ε model = 1.92]

C_3 : Constant in ε Equation Buoyancy Terms [Default value in standard k-ε model = 0.0]

c_p : Specific Heat

G : Production due to Buoyancy Force
g : Gravitational Acceleration
H : Total Enthalpy
K : Area Porosity Tensor
k : Turbulence Kinetic Energy
P : Modified Pressure
P' : Thermodynamic Pressure
P_s : Shear Production
Q : Heat Source or Sink in Porous Medium
R : Resistance in Porous Medium
T : Temperature
t : Time
U : Fluid Velocity

Greek

Γ_e : Effective Diffusivity
γ : Volume Porosity
Δ : *Difference*
∇ : Derivative
ϵ : Turbulent Dissipation Rate
ξ : Bulk Viscosity
λ : Thermal Conductivity
μ : *Laminar Viscosity*
μ_{eff} : Effective Viscosity
μ_t : Turbulent Viscosity
ρ : Density
σ_k : Turbulent Prandtl Number for k
σ_ϵ : Turbulent Prandtl Number for k
σ_ρ : Turbulent Prandtl Number for density

Reference

1. D. J. Lee, "Development of Fluid System Design for Small and Medium integral Reactor", KAERI/RR-1722/96 (1996).
2. Y. Y. Bae, "Development of Essential System Technologies for Advanced Reactor", *KAERI/RR-1882/98 (1998).*
3. D. J. Lee, "A Study of Passive and Inherent Safety Design Concepts for Advanced Light Water Reactors," KAERI/CM-112/96, KAERI (1996).
4. "The Status of R&D for Nuclear Ship Reactor", JAERI (1992/1993) (Translated to Korean)
5. "N. S. Savannah Safety Assessment, Vol. 1, Engineering and Construction", Babcock & Wilcock Co., Atomic Energy Div. (1960) ; "N. S. Savannah Safety Assessment, Vol. 2, Operations", State Marine Lines. (1961).
6. M. Konb, Kest berichte Nr. 31, Verag Karl Thiemig, Munchen (1983).
7. N. Isshiki, "Effects of Heaving and Listing upon Thermo-hydraulic Performance and Critical Heat Flux of Water-cooled Marine Reactors," Nucl. Eng. Des., 4, 138 (1966).
8. T. Otsuji and A. Kurosawa, "Critical Heat Flux of Forced Convection Boiling in an Oscillating *Acceleration Field - I. General Trends,*" Nucl. Eng. Des., 71, 15 (1982).
9. T. Ishida, "Experiments of Two-phase Flow Dynamics of Marine Reactor Behavior under Heaving Motion," Nucl. Sci. and Tech., 34(8), *771 (1997).*
10. I. Iyori, "Natural Circulation of Integrated-type Marine Reactor at Inclined Attitude," Nucl. Eng. Des., 99, 423 (1987).
11. I. Iyori, F. Inasaka, T. Matsuoka, and I. Aya, "Basic Flow Rate Characteristics of Natural Circulation of Marine Reactors at Inclined Attitude," 2nd International Topical Meeting on Nuclear Power Plant Thermal Hydraulics and Operations, Tokyo, Japan, April 15-17, *p.1-124 (1986).*
12. H. Murata, " Natural Circulation Characteristics of a Marine Reactor in Rolling Motion," Nucl. Eng. Des., 118, 141 (1990).
13. "CFX 4.2 Manual", AEA (1997).
14. J. H. Kim, S. M. Lee and G. C. Park, "Study on the Natural Circulation Characteristics of Integral Type Reactor for Vertical and

Inclined Conditions", The 15th International Conference on the Structural Mechanics in Reactor Technology(SMiRT-15) (1999).
15. M. Ishii and I. Kadaoka, "Scaling Laws for Thermal-hydraulic System under Single Phase and Two-phase Natural Circulation," Nucl. Eng. Des., 81, 411 (1984).
16. G. Kocamustafaogullari and M. Ishii, "Scaling of Two-phase Flow Transients using Reduced Pressure System and Simulant Fluid," Nucl. Eng. Des., 104, 121 (1987).
17. N. E. Todreas and M. S. Kazimi, "Nuclear System II: Elements of Thermal
18. "Using CFX-4 with CFX-Build", AEA (1996).
19. S. V. Patankar, "Numerical Heat Transfer and Fluid Flow", Hemisphere Publishing Co. (1980).